

Extraction of The Parameters of A Photovoltaic Solar Cell by A Metaheuristic Method Associated With The Lambert-W Function

Steve NGOFFE PERABI
Higher Teachers' College of Bertoua
University of Bertoua
Bertoua, Cameroon

Pierre KENFACK
Department of Electrical and Power Engineering
Higher Teachers' Training College (HTTC)
Buea, Cameroon

Abraham DANDOOUSSOU
Department of Electrical and Power Engineering
Higher Teachers' Training College (HTTC)
Buea, Cameroon

Francelin Edgar NDI
Technology and Applied Sciences Laboratory
University of Douala
Douala, Cameroon

Nicaire NDONGMO FOTSA
Technology and Applied Sciences Laboratory
University of Douala
Douala, Cameroon

Aristide TOLOK
Higher Teachers' Training College of Ebolowa
University of Ebolowa
Ebolowa, Cameroon

Grégoire ABESOLO ONDOUA
Ecosystems and Fisheries Resources Laboratory
University of Douala
Douala, Cameroon

Salomé NDJAKOMO ESSIANE
Cameroonian Association for Research and Innovation in
Energy and Environmental Technology (ACRITE)
University of Ebolowa
Ebolowa, Cameroon

Abstract — The design of a PV system involves establishing a PV model that faithfully and accurately reproduces the actual behaviour of the system under various conditions. The accuracy of this model is proportional to the parameters extracted by optimization methods, generally metaheuristic methods. Referring to the literature, we have identified two methods for calculating the estimated current based on the objective function. The first step was to determine the most efficient method for calculating the estimated current, with a view to obtaining the most consistent and accurate solutions. The algorithms used were Monarch Butterfly Optimization and Social Spider Optimization. Experimental data from the RTC France solar cell were used in this case study. The main results show that the iterative method based on the Lambert function for calculating the estimated current in the objective function provides more accurate and precise solutions than the approximate method using the measured current to determine the estimated current. What's more, the Monarch Butterfly Optimization algorithm provides more accurate solutions than many other methods in the literature.

Keywords— *Extraction, Parameters, Metaheuristic method, Lambert W*

I. INTRODUCTION

The unrestrained race of man towards the development of infrastructure, allowing the improvement of his standard of living, pushed this last one to develop a diagram of energy production that mainly leaned on fossil fuels [1]. It is estimated that more than 71% of the world's electricity production is based on fossil fuels [2]. This pattern of production, if it is maintained, will inexorably lead to numerous consequences for both humans and the environment [3]. Many organizations, in accordance with the climate protocol, have opted to migrate to renewable energies. These have many advantages, including reduced pollution, environmental friendliness, and the infinite availability of the primary source [4, 5]. Among the renewable sources, we can mention wind, water, biomass, and the sun. This last one is one of the most accessible renewable energy sources on the globe [6]. With a rapidly increasing growth rate, the energy production of solar photovoltaic (PV) installations in recent years has risen from 89.5 GW in 2012 to over 800 GW today [7]. There are many areas of application for this form of energy. These include telecommunications [8], the military [9], and increasingly the automotive sector [10, 11].

Nevertheless, this production scheme is more sensitive to external factors [12]. In order to efficiently and accurately predict electricity production from solar PV modules while optimizing and controlling photovoltaic systems, mathematical models have been developed [13]. Among others, we can mention the single-diode model, the double-diode model, and, more recently, the three-diode model for industrial configurations [14]. These models are characterized

by parameters that must be accurately estimated. Obtaining these different parameters remains a crucial and primary problem. This is due to the transcendence of the current-voltage characteristic equation, which makes it difficult to solve because it leads to an optimization problem. In the literature, several methods have been identified for the extraction of the best parameters of a PV cell or module. The application of these methods shows that the accuracy obtained from the results is different from one method to another [15].

Analytical methods are the most commonly used methods to extract the parameters of a PV module. The advantages of this method are the speed of calculation and the relative accuracy of the results, as only one analytical equation is needed to obtain the solution of a parameter [16]. However, despite the popularity of this method, it is not always easy to apply because it requires many data points on the curve, which makes the calculation more complex [17]. They are effective for some PV module models under standard test conditions (STC) as well as under other environmental conditions. Batzelis et al [18] have expressed the voltage as a function of current using Lambert's W function. Therefore, this method combines the versatility and accuracy provided by the single-diode model with a faster and more robust execution. Bai et al [19] proposed a new method consisting of a piecemeal adjustment combined with the four-parameter model to simplify the calculation procedures to obtain the five parameters. Femia et al [20] proposed a method to analytically calculate the series resistance R_s and the parallel resistance R_{sh} using Lambert's W function. This method explicitly expresses the output current of the PV module as a function of the voltage, and shows good performance. Metaheuristics or intelligent methods using artificial intelligence techniques are increasingly used to estimate PV module parameters because of their reliability and performance. These numerical methods with curve-fitting techniques are better than analytical methods. The algorithms of these methods provide accurate results by evaluating all points of the current-voltage curve [21]. These global optimization methods do not impose any restrictions on the problem formulation and have the ability to solve various complex problems [13]. Many works are based on some of the evolutionary algorithms. Harrag et al [22] use the genetic algorithm (GA) to extract the parameters of a PV cell subjected to varying temperature conditions. Allam et al [23] proposed the Flower Pollination Algorithm (FPA), which has the quality of quickly converging to the optimal solution of single and dual diode PV module parameters. This method is simple, highly efficient, and outperforms GA methods. Muhsen et al [24] estimate the parameters with the Differential Evolution with Adaptive Mutation (DEAM) algorithm. This algorithm uses the notion of attraction-repulsion to improve on the original differential evolution (DE) mutation operation, a method that provides high

accuracy, fast convergence, and optimally fitted control parameters. Jordehi et al [25] use a hybrid variant of the particle swarm optimization (PSO) algorithm to extract the parameters of a PV solar cell. This method has high sensitivity to the initial parameters. Abd Elaziz et al [26] use a variant of the Whale Optimization Algorithm (WOA) for the extraction of the intrinsic parameters of a PV solar cell. This method has been shown to be efficient in estimating the parameters of a PV cell, but its limitations are its sensitivity to the starting parameters and a relatively long computation time. Ayang et al [27] and [28], use the maximum likelihood estimator (MLE) and least squares estimator (LSE) to extract the parameters of the single diode PV module under standard test conditions. Ndongmo et al [29] use the bald eagle algorithm (BES) for the estimation of the internal parameters of a PV cell. This method shows its accuracy in parameter estimation, but the method is very sensitive to the initial parameters. Ndi et al [30] proposed the equilibrium optimizer algorithm to estimate the parameters of a photovoltaic solar cell. This method has shown its effectiveness in solving this type of problem. However, it is very sensitive to the initial parameters.

Evaluating the performance of metaheuristic optimization algorithms relies on a number of factors. One of the most widely used factors is the root mean square error. This is the difference between the measured current and the estimated current [31]. According to the literature, this error can be evaluated using either an iterative method (using numerical resources to solve the nonlinear equation of the cell model with the extracted parameters), or an approximate method (the measured current and the extracted parameters are used to calculate the estimated current) [32].

In this manuscript, both methods of calculating the estimated current are employed with new optimization algorithms. The aim is to determine the most accurate method for providing a reliable and precise PV model. Here, we propose two estimation methods, to extract the parameters of the single-diode model (SDM) and the double-diode model (DDM). These methods are the Social Spider Optimization (SSO) method and the Monarch Butterfly Optimization (MBO) method. We test the proposed work on a well-known dataset, the R.T.C. France commercial solar cell dataset, and then compare the proposed methods with selected algorithms to verify their effectiveness. The results of the proposed algorithms have been validated by Lambert equations for SDM and DDM.

The main contributions of this paper are presented as follows:

- A comparison between the proposed methodologies for calculating the estimated current is established to determine which is the most robust, reliable, and

accurate whatever the proposed algorithm.

- Two new optimization algorithms (SSO and MBO) have been used to identify SDM and DDM parameters based on experimental data sets measured under different environmental conditions.
- A comparison between the RMSE obtained by the optimizers and the RMSE calculated on the basis of the Lambert function was reported as evidence of the accuracy of the identification.
- Finally, a comparison is made with existing literature in order to position our work in relation to what already exists.

This article is organized as follows: First, we present the generalities concerning the modelling of a PV solar cell. Then, a second time, we will focus on the extraction method used. We will present the results of this method, and then we will finish with a conclusion.

II. MODELLING OF A PV SOLAR CELL

In the literature, the single-diode model is the simplest and most widely used model. This is justified by its precision in the parameters obtained, its speed in execution, and especially its simplicity in the implementation of its structure [33]. The equivalent electrical diagram is given in Fig. 1.

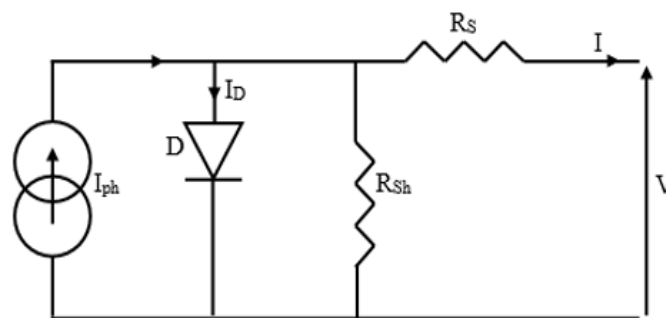


Fig. 1: Single Diode Model

By applying Kirchhoff's theorem to this circuit, we can establish the expression of the current I of the PV solar cell as a function of the voltage V , which is given by equation (1):

$$I = I_{ph} - I_0 \left(e^{\frac{q(V+IR_S)}{nKT}} - 1 \right) - \frac{(V+IR_S)}{R_{Sh}} \quad (1)$$

Where I_{ph} is the photo current, I_0 is the saturation current of the diode, n is the ideality factor, K is the Boltzmann constant, q is the charge of the electron, T is the temperature of the module, R_S is the serial resistance, and R_{Sh} is the shunt resistance.

This model has five unknown parameters, namely: the photo current (I_{ph}), the saturation current of the diode (I_0), the shunt resistance (R_{Sh}), the series resistance (R_S), and the ideality factor of the diode (n). These last ones, chosen in an optimal way, allow, in addition to efficiently predicting production, to successfully adapt to a certain extent to the experimental data. However, studies have shown that this model inherently neglects the recombination current losses in the depletion region of the junction diode, resulting in a deterioration of accuracy at low irradiances [34]. Taking into account this loss, especially in open circuits, leads to a more accurate solution [35]. Thus, the double-diode model, as shown in Fig. 2, uses one diode as a rectifier while the other addresses the loss due to the recombination current [30].

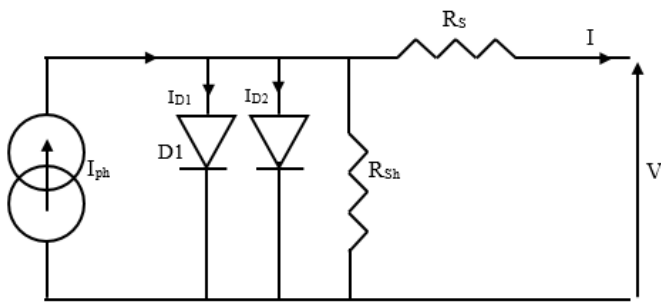


Fig. 2: Double Diode Model

By applying Kirchhoff's theorem to this circuit, we can establish the expression of the current I of the PV solar cell as a function of the voltage V , which is given by the equation (2):

$$I = I_{ph} - I_{01} \left(e^{\frac{q(V+IR_S)}{n_1KT}} - 1 \right) - I_{02} \left(e^{\frac{q(V+IR_S)}{n_2KT}} - 1 \right) - \frac{(V+IR_S)}{R_{Sh}} \quad (2)$$

This model requires the knowledge of seven unknown parameters, namely: the photo current (I_{ph}), the saturation current of diode 1 (I_{01}), the saturation current of diode 2 (I_{02}), the shunt resistance (R_{Sh}), the series resistance (R_S), the ideality factor of diode 1 (n_1), and the ideality factor of diode 2 (n_2). The Double-diode model, compared to the one-diode model, significantly improves the accuracy of the PV system [13]. Nevertheless, it presents additional computations and complexity in the intrinsic parameters.

III. OBJECTIVE FUNCTION CALCULATION

Each equation of the above-mentioned electrical models can be treated as an optimization problem. For this purpose, it

is necessary to have a data set. The objective function allows you to check if the result produced by a set of parameters is close to the required values provided in the data set. The minimization of the root mean square error (RMSE) is the objective function par excellence. Here, the objective is to minimize the difference between the measured and estimated currents. The optimization techniques are based on the principle of identifying the best vector X that minimizes the objective function [14].

Thus, the expression of the objective function (Obj_1) is given by equation (3):

$$Obj_1 = \text{Min} \left(\sqrt{\frac{1}{N} \sum_{k=1}^N (I_{k,meas} - I_{k,est}(V_k, I_k, X))^2} \right) \quad (3)$$

Where:

- N is the number of points measured.
- $I_{k,meas}$ is the current measured.
- $V_{k,meas}$ is the voltage measured.
- $I_{k,est}(X)$ is the current estimated by the metaheuristic method with the equation (1) for the SDM and the equation (2) for the DDM.
- X is the intrinsic parameter obtained with the metaheuristic method.

However, this mathematical expression of the mean square error is not correct. The expression of the estimated current is a function of the measured current and voltage. Thus, the result given by equation (3) will not reflect the real value of the error. Thus, the proposed iterative procedure for calculating the estimated current for a single-diode model can be formulated by the Lambert-W equation [36, 37]:

$$y = w(\alpha) \quad (4)$$

With

$$\alpha = \frac{\frac{nR_S}{V_t}}{1 + \frac{R_S}{R_{Sh}}} \left(I_0 \exp\left(\frac{nV_{mes}}{V_t}\right) \exp\left(\frac{nR_S}{V_t}\right) \left(\frac{I_{ph} + I_0 - \frac{V_{mes}}{R_{Sh}}}{1 + \frac{R_S}{R_{Sh}}} \right) \right) \quad (5)$$

Where

$$V_t = \frac{nKT}{q} \quad (6)$$

Based on equation (4), the expression for the estimated current given by equation (1) can be rewritten as follows:

$$I_{Lam} = \frac{I_{ph} + I_0 - \frac{V_{mes}}{R_{Sh}} - \frac{y(1 + \frac{R_S}{R_{Sh}})}{\frac{nR_S}{V_t}}}{1 + \frac{R_S}{R_{Sh}}} \quad (7)$$

The proposed iterative procedure, based on the Lambert W function, for computing the estimated current for a double-diode model can be formulated as follows [36].

$$\theta = \alpha + \beta \exp(\Delta) \quad (8)$$

$$y = w(\theta) \quad (9)$$

Where

$$\alpha = \frac{\frac{n_1 R_S}{V_t}}{1 + \frac{R_S}{R_{Sh}}} \left(I_{01} \exp\left(\frac{n_1 V_{mes}}{V_t}\right) \exp\left(\left(\frac{n_1 R_S}{V_t}\right) \left(\frac{I_{ph} + I_{01} + I_{02} - \frac{V_{mes}}{R_{Sh}}}{1 + \frac{R_S}{R_{Sh}}}\right)\right) \right) \quad (10)$$

$$\beta = \frac{\frac{n_1 R_S}{V_t}}{1 + \frac{R_S}{R_{Sh}}} \left(I_{02} \exp\left(\frac{n_2 V_{mes}}{V_t}\right) \exp\left(\left(\frac{n_2 R_S}{V_t}\right) \left(\frac{I_{ph} + I_{01} + I_{02} - \frac{V_{mes}}{R_{Sh}}}{1 + \frac{R_S}{R_{Sh}}}\right)\right) \right) \quad (11)$$

$$\Delta = 1 - \frac{n_1}{n_2} \quad (12)$$

Based on equation (8), we can rewrite the equation as follows:

$$I_{Lam} = \frac{I_{ph} + I_{01} + I_{02} - \frac{V_{mes}}{R_{Sh}} - \frac{y(1 + \frac{R_S}{R_{Sh}})}{\frac{n_1 R_S}{V_t}}}{1 + \frac{R_S}{R_{Sh}}} \quad (13)$$

Thus, the new objective function formulation (Obj2) of the root mean square error is given by equation (14) as follows:

$$Obj_2 = \text{Min} \left(\sqrt{\frac{1}{N} \sum_{k=1}^N \left(I_{k,mes} - I_{k,Lam}(V_k, X) \right)^2} \right) \quad (14)$$

IV. OPTIMIZATION METHODS

In this section, we will present the metaheuristic optimization methods used in the rest of our work.

A. Monarch Butterfly Optimization

Feng et al. [38] proposed a new optimization approach based on swarm intelligence in 2015. Monarch Butterfly Optimization (MBO) is inspired by the migration behaviour of monarch butterflies from one continent to another, i.e., monarch butterfly optimization (MBO). Fig. 3 shows the movement of the monarch butterfly from one region to another. They keep their reproduction cycle active during this cross-county movement [39].

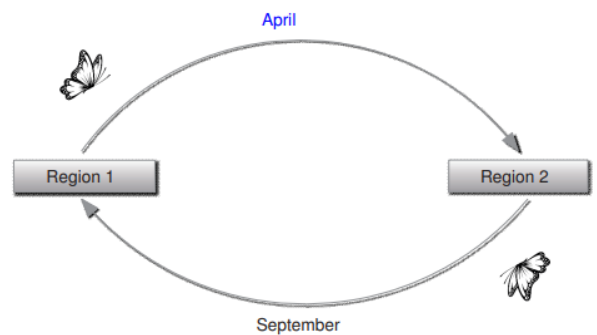


Fig. 3: Migratory behaviour of the monarch butterfly [38]

The migration behaviour is modelled into some mathematical formulation.

A collection of pre-defined criteria is developed in order to represent the realistic migration behaviour of monarch butterflies. The following are the pre-defined rules [38].

- All members of the monarch fleet should be in either region 1 or region 2. In MBO, the total population is regarded as representing the whole population of that region.
- The migration operator, which can be regulated by the migration ratio, produces new offspring of monarch butterflies in regions 1 or 2.
- The overall population of monarch butterflies stays unchanged in MBO. If the children outperform their parents in terms of fitness, they take over.
- The flutter's fittest butterfly remains in the fleet and is unaffected by the migration operator.

Monarch butterflies move from area 1 to region 2 every year in April and return in September, as seen in Fig. 3. Monarch butterflies are seen to fly in Region 1 from September to March and in Region 2 from April to August. Assume that the number of monarch butterflies remaining in region 1 is referred to as subpopulation 1' and is denoted by P_{n1} . P_{n1} is defined as the nearest integer larger than or equal to R .

$$R = P_n \times P_{n1} \quad (15)$$

Where R and P_n are the ratios of butterfly flutter remaining in region 1 and the total monarch butterfly population, respectively. Similarly, butterflies located in Region 2 are classified as subpopulation 2.

$$P_{n2} = P_n - P_{n1} \quad (16)$$

This butterfly migratory mechanism is mathematically represented as:

$$S_{i,j}(t+1) = S_{r1,j}(t) \quad (17)$$

With

$S_{i,j}(t+1)$ denotes the j^{th} position element or variable of the i^{th} butterfly in the $t+1$ generation, whereas $S_{r1,j}(t)$ denotes the j^{th} element of S_{r1} , which is the new location of monarch butterfly $r1$ in the current generation t . The butterfly $r1$ is chosen at random from subpopulation 1 or region 1.

A random number r is created for decision-making purposes as follows:

$$r = \gamma \times rand \quad (18)$$

Where $rand$ is a random integer drawn from a uniform distribution and γ is the migration period, believed to be 1.2 for 12 months. If $r \leq R$, then equation (17) produces the new element j of the butterfly; otherwise, the new-born monarch butterfly is formed as

$$S_{i,j}(t+1) = S_{r2,j}(t) \quad (19)$$

Where $r2$ is a randomly chosen monarch butterfly from subpopulation 2 or region 2. The direction of migration can be adjusted by altering the value of R . For example, if R is high, more monarch butterflies P_{n1} members are predicted. A low R value, on the other hand, increases the number of P_{n2} monarch butterflies in subpopulation 2 or region 2. The selection of R is critical in order to develop new monarch butterflies.

B. Social Spider Optimization

Cuevas et al. [40] presented the Social Spider Optimization algorithm (SSO), a modern population-based swarm intelligence system. The social behaviour of the social spider colony, which comprises social individuals and a common web, inspired the SSO algorithm. Because of its efficiency, the SSO has been used in a variety of applications, particularly for solving global optimization issues [41].

Female and male spiders account for 70% and 30% of total colony members, respectively [42]. Each member of the colony is responsible for a separate task, such as building and maintaining the common web, catching prey, using water, and so on[43]. Female spiders either attract or repel others. The community web vibrations are dependent on the weight and distance of the limbs, which are the primary aspects of a spider's attraction or aversion [44]. Male spiders are classified into two types: dominant and non-dominant [45].

Dominant male spiders are physically superior to non-dominant spiders. The dominant male may mate with one or all of the females in the colony in order to share knowledge and create progeny. The method for optimizing each solution in the spider social optimization (SSO) algorithm symbolizes a spider location, while the common web represents the search space. Each solution's value is expressed by computing its fitness function, which represents each spider's weight. Each spider's weight.

The population in the SSO method consists of N_s solutions (spiders) and may be classified into females f_i and males m_i . The number of females N_f is chosen to be between 65% and 90% and may be estimated using the following equation (20):

$$N_f = \text{floor}((0.9 - rand(0,1)) \cdot 0.25) \cdot N_s \quad (20)$$

With $rand$ is a random number between (0, 1) and $\text{floor}(\cdot)$ converts a real number to an integer number. The number of male spiders N_m can be calculated as follows:

$$N_m = N_s - N_f \tag{21}$$

The female and male spider position f_i and m_i are randomly generated within the lower LB and the upper UB initial parameter bounds as follows.

$$f_{i,j}^0 = LB + rand(0,1). (UB - LB) \tag{22}$$

$$m_{k,j}^0 = LB + rand(0,1). (UB - LB) \tag{23}$$

With

$$i = \{1, 2, 3, \dots, N_f\} \quad , \quad k = \{1, 2, 3, \dots, N_m\} \quad \text{and} \quad j = \{1, 2, 3, \dots, n\}$$

The zero signals represent the initial population and i, j and k are the parameter and individual indices, respectively. The value of f_i, j is the j^{th} parameter of the i^{th} female spider position.

The weight of each spider represents the quality of the answer. The fitness function value of each solution I is calculated as follows.

$$w_i = \frac{J(s_i) - worst_s}{best_s - worst_s} \tag{24}$$

Where $J(s_i)$ is the fitness value of the spider position, s_i with regard to the substituted objective function $J(\cdot)$. The value $worst_s$ represents the maximum solution's value while the $best_s$ represents the minimum value of the solution in the population. These values are defined by considering the following minimization problem as follows.

$$best_s = \min J(s_k) \text{ and } worst_s = \max J(s_k) \tag{25}$$

With $k = \{1, 2, 3, \dots, N_s\}$.

The transmission of the information by the colony members is done through the communal web by encoding it as small vibrations. The vibrations perceived by the solution i from solution j is modelled by the equation (26).

$$vib_{i,j} = w_j \cdot e^{-a_{ij}^2} \tag{26}$$

The dominant male is responsible for mating of female members when it locates them with a specific range rm . This operation can be calculated as follows

$$r_m = \sum_{j=1}^n \frac{p_j^{high} - p_j^{low}}{2.n} \tag{27}$$

V. RESULTS

The framework of this section is divided into subsequent subsections; the first one concerns the comparison among the objective functions across the implemented algorithms, while the second one focuses on detecting the superior algorithm. For this extraction, we used the Matlab R2020a platform. This was simulated on a computer with the following specifications: an Intel Core i5-3437U @ 1.9 GHz, 8 GB of RAM, and the Windows 10 64-bit operating system.

TABLE I. shows the upper and lower bounds, for each unknown parameter in each PV model.

TABLE I. Lower and Upper bounds

Parameters	Lower bound	Upper bound
$I_{ph} (A)$	0	1
$I_0, I_{01}, I_{02} (\mu A)$	0	10-6
$R_s (\Omega)$	0	0,5
$R_{sh} (\Omega)$	0	100
$n, n1, n2$	1	2

A. Comparison among the proposed objective functions

In this section, a well-regarded dataset of RTC France solar cells is utilized to compare the two reported objectives of Equations. 3 and 14. The proposed algorithms are executed to identify the parameters of SDM and DDM for the cell based on the measured dataset at an irradiance of 1000W/m2 and a temperature of 33°C. These experimental values of the output voltage and current of an RTC France are found in a lot of manuscripts in particular [13] and [29].

1) Extraction for a single diode model (SDM)

This paragraph summarizes the outcomes of the algorithms investigated in this research utilizing the SDM and the goal functions described in Equations 3 and 14. Table 2 shows the results of the Lambert function's RMSE calculation, which includes the difference between the Obj1 and Obj2.

According to the results from Table 2, we see that after 500 iterations, the Lambert-W function allows us to refine the estimation of the root mean square error. Thus, we go from an RMSE equal to 48.977×10^{-4} using the equation (3) to an RMSE equal to 46.0517×10^{-4} with the equation (14) for the Social Spider Optimization (SSO) method and from 10.111×10^{-4} RMSE to 7.8028×10^{-4} using the Monarch Butterfly Optimization (MBO) method with the Lambert W function. It is also important to underline the superiority in terms of accuracy of the MBO algorithm compared to the SSO algorithm. This algorithm minimizes the Obj1 function, as well as the Obj2 function. This shows that the current estimated by this method is closest to the measured current. The intrinsic parameters of this method are much closer to the results presented in the literature. Fig. 4 shows the performance of the parameter estimation by the SSO method associated with the Lambert-W function for a single-diode model.

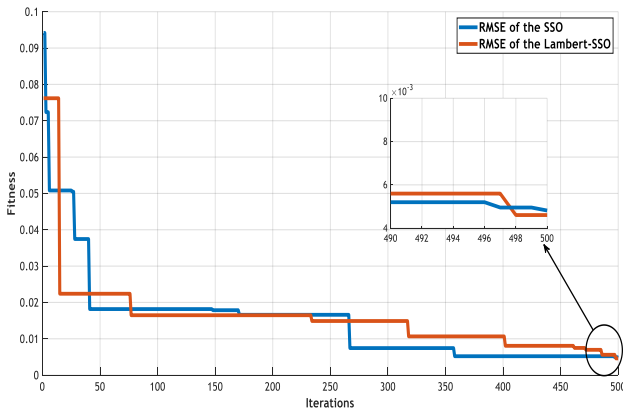


Fig. 4: Convergence of the SSO and Lambert SSO methods to the optimal solution.

2) Extraction for a double diode model (DDM)

This paragraph summarizes the outcomes of the algorithms investigated in this research utilizing the DDM. Table 3 shows the results of the Lambert function's RMSE calculation, which includes the difference between the Lambert RMSE (Lambert RMSE) and the values produced by Obj1 and Obj2.

For 100 iterations, we find that the MBO algorithm is significantly more accurate than the SSO algorithm. This algorithm minimizes more of the Obj1 function, demonstrating that the current estimated by this method is close to the measured current. The intrinsic parameters of this method are much closer to the results found in the literature. Regarding the objective function Obj2, we observe that, compared to the SSO algorithm, the MBO algorithm minimizes the most the difference between the measured current and the estimated current. The Lambert-W function associated with the latter allows for further refinement of the estimation of the internal parameters of the model, as shown in Fig. 5.

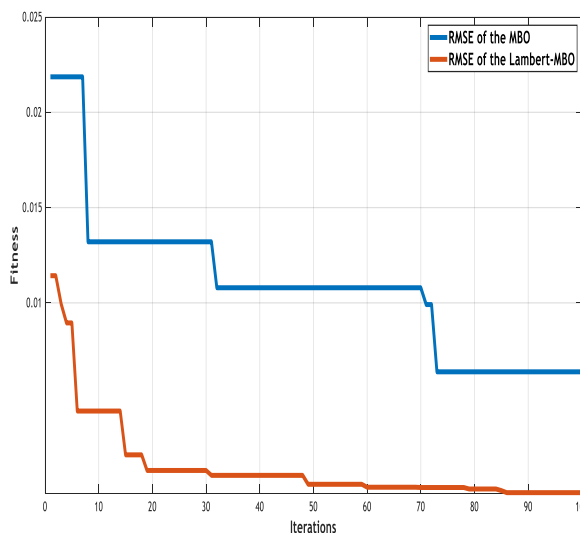


Fig. 5: Convergence of the MBO and Lambert MBO methods to the optimal solution

Fig. 5 shows the performance of parameter estimation by the MBO method associated with the Lambert-W function before the standard MBO method.

B. Comparison results with the literature

Tables 2 and 3 have shown the superiority and accuracy of computing the mean square error by the W-Lambert function. It appears that this function is more efficient and accurate in the evaluation of the objective function. In this part, we compare the results of the use of the Lambert-W function for a model with single and double diodes with the results found in the literature.

The results resulting from the comparison of these methods with those in the literature for a commercial solar cell RTC France under the conditions described upstream are presented in Table 4. In the latter, we can observe the

superiority of the Monarch Butterfly Optimization method ($RMSE_{MBO} = 7.802 \times 10^{-4}$) for the extraction of the parameters of a single diode model, compared to the numerous algorithms listed in the literature. This method thus outperforms methods such as the Parasitism Predation Algorithm ($RMSE_{PPA} = 9.503 \times 10^{-4}$), the Slime Mould Algorithm ($RMSE_{SMA} = 11.712 \times 10^{-4}$), the Harris Hawks Optimizer ($RMSE_{HHO} = 21.607 \times 10^{-4}$) and the Social Spider Optimization ($RMSE_{SSO} = 46.051 \times 10^{-4}$). This superiority is due to a greater ability to explore and exploit than with the methods cited above. However, this method is less accurate than the Marine Predator Algorithm ($RMSE_{MPA} = 7.7301 \times 10^{-4}$) due to population diversity.

Fig. 6 shows the I-V characteristic curve of the photovoltaic cell, derived from the measured data (red dot curve) and the intrinsic parameters extracted from the cell by the Lambert-MBO method (blue dot curve) and the Lambert-SSO method (green curve) under the test conditions mentioned above.

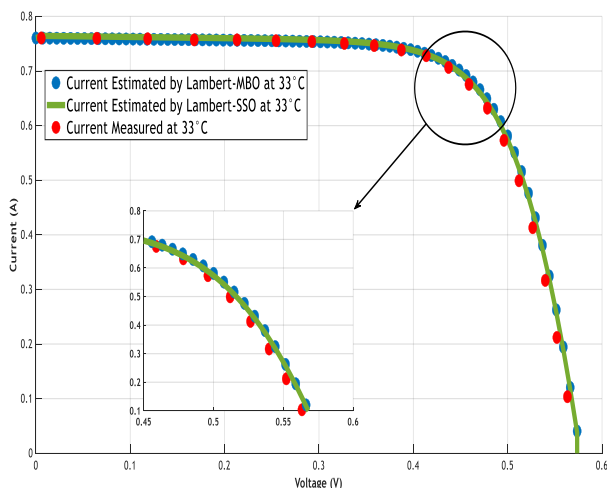


Fig. 6: I-V characteristic of the SDM.

For a double-diode model, the results from the comparison of these methods with those in the literature, for a commercial RTC France solar cell, under the conditions described above, are presented in Table 5. In the latter, we note the effectiveness of the Monarch Butterfly Optimization ($RMSE_{MBO} = 6.352 \times 10^{-6}$) and Social Spider Optimization ($RMSE_{SSO} = 3.943472 \times 10^{-5}$) methods for extracting the parameters of a double-diode model. These surpass in accuracy and efficiency many algorithms listed in the scientific literature. These methods demonstrate their effectiveness in solving this problem with high nonlinearity, because they have a greater capacity for exploration and exploitation than the algorithms listed in the literature. They

outperform the Chaotic Lambert Success History Based Adaptive Differential Evolution method ($RMSE_{Chaotic-LSHADE} = 7.5274 \times 10^{-4}$), the Marine Predator Algorithm ($RMSE_{MPA} = 7.7696 \times 10^{-4}$), the Slime Mould Algorithm ($RMSE_{SMA} = 9.9715 \times 10^{-4}$), the Parasitism Predation Algorithm ($RMSE_{PPA} = 11.172 \times 10^{-4}$), and the Harris Hawks Optimizer ($RMSE_{HHO} = 12.491 \times 10^{-4}$) which presents the least accurate results in the extraction of the parameters.

These results show that the Monarch Butterfly Optimization (MBO) algorithm was able to effectively extract the parameter values to concretely predict the measured curve in a meaningful way. The Social Spider Optimization (SSO) method is more accurate in extracting the intrinsic parameters for the double-diode model than for the single-diode model.

VI. CONCLUSION

Renewable energy resources are a critical topic that can help tackle many energy-related issues. This type of energy has the potential to overcome numerous difficulties associated with the existing production system, which is mostly focused on fossil fuels. Solar energy is seen as the best solution to solving the difficulties related to fossil fuels owing to its availability and ease of deployment. In order to efficiently predict electricity production while optimizing PV systems, PV models have been developed. In order to extract precise and accurate parameters from PV models, it is necessary and even imperative to have a reliable objective function and a robust algorithm. This can be estimated either iteratively or by approximation by linearly solving the estimated current as a function of the measured current. In this manuscript, we have presented the accuracy of the methods discussed in the literature and established the most reliable and accurate method for extracting SDM and DDM model parameters. Relying on an objective function based on an iterative method, diode model parameter extraction provides more accurate, precise, and reliable solutions than the approximate method. This has been verified regardless of which algorithm is highlighted here. The MBO algorithm has shown its superiority over SSO and many other algorithms in the literature in terms of stability, optimal solution matching, and error curve convergence. However, despite the highlighted performance in terms of precision and accuracy of the optimal solution, the iterative method has a longer computation time than the approximate method.

VII. REFERENCES

- [1] R. Adib et al., "Renewables 2015 global status report," REN21 Secretariat, Paris, France, vol. 162, 2015.
- [2] D. Raimi, E. Campbell, R. Newell, B. Prest, S. Villanueva, and J. Wingeno, "Global Energy Outlook 2022: Turning Points and Tension in the Energy Transition," Resources for the Future Report, Washington, DC, 2022.
- [3] N. Matera, D. Mazzeo, C. Baglivo, and P. M. Congedo, "Climate Change Will Affect Photovoltaic Performances? A Long-Term Analysis from 1971 to 2100 in Italy," *Energies*, vol. 15, no. 24, p. 9546, 2022.
- [4] F. F. Amigue, S. N. Essiane, S. P. Ngoffe, and A. T. Nelem, "Optimal Placement and Sizing of Distributed Energy Generation in an Electrical Network Using the Hybrid Algorithm of Bee Colonies and Newton Raphson," *Journal of Power and Energy Engineering*, vol. 8, no. 6, pp. 9-21, 2020.
- [5] R. F. Bella, S. N. Essiane, S. K. Nghoh, and B. Fouotsap, "Variability of Performance Indices of Photovoltaic Solar Panels in Operating Conditions in the Littoral Zone of Cameroon," *Computational Water, Energy, and Environmental Engineering*, vol. 10, no. 3, pp. 108-116, 2021.
- [6] G. M. Mengata, S. N. Perabi, F. E. Ndi, and Y. S. Wiysahnyuy, "Characterization of solar photovoltaic modules powered by artificial light for use as a source for smart sensors," *Energy Reports*, vol. 8, pp. 12105-12116, 2022.
- [7] M. J. N. Matip, S. N. Essiane, S. P. Ngoffe, and Y. C. K. Mougang, "Estimation of wind power in coastal areas using a Model based on the learning of a Multilayer Perceptron: Case of Douala, Cameroon," in *E3S Web of Conferences*, 2022, vol. 354, p. 01009: EDP Sciences.
- [8] U. Gangopadhyay, S. Jana, and S. Das, "State of art of solar photovoltaic technology," in *Conference papers in science*, 2013, vol. 2013: Hindawi.
- [9] A. Rahman et al., "Sub-50-nm self-assembled nanotextures for enhanced broadband antireflection in silicon solar cells," *Nature communications*, vol. 6, no. 1, p. 5963, 2015.
- [10] A. Singh and S. S. Letha, "Emerging energy sources for electric vehicle charging station," *Environment, Development and Sustainability*, vol. 21, pp. 2043-2082, 2019.
- [11] D. Mazzeo, N. Matera, R. De Luca, and R. Musmanno, "A smart algorithm to optimally manage the charging strategy of the Home to Vehicle (H2V) and Vehicle to Home (V2H) technologies in an off-grid home powered by renewable sources," *Energy Systems*, pp. 1-38, 2022.
- [12] L. Lu, T. Zheng, Q. Wu, A. M. Schneider, D. Zhao, and L. Yu, "Recent advances in bulk heterojunction polymer solar cells," *Chemical reviews*, vol. 115, no. 23, pp. 12666-12731, 2015.
- [13] F. E. Ndi, S. N. Perabi, S. E. Ndjakomo, and G. O. Abessolo, "Harris Hawk Optimization Combined with Differential Evolution for the Estimation of Solar Cell Parameters," *International Journal of Photoenergy*, vol. 2022, 2022.
- [14] D. Yousri, D. Allam, M. Eteiba, and P. N. Suganthan, "Static and dynamic photovoltaic models' parameters identification using chaotic heterogeneous comprehensive learning particle swarm optimizer variants," *Energy conversion and management*, vol. 182, pp. 546-563, 2019.
- [15] T. Ayodele, A. Ogunjuyigbe, and E. Ekoh, "Evaluation of numerical algorithms used in extracting the parameters of a single-diode photovoltaic model," *Sustainable Energy Technologies and Assessments*, vol. 13, pp. 51-59, 2016.
- [16] R. Tamrakar and A. Gupta, "A Review: extraction of solar cell modelling parameters," *International journal of innovative research in electrical, electronics, instrumentation and control engineering*, vol. 3, no. 1, pp. 55-60, 2015.
- [17] D. Kler, P. Sharma, A. Banerjee, K. Rana, and V. Kumar, "PV cell and module efficient parameters estimation using Evaporation Rate based Water Cycle Algorithm," *Swarm and evolutionary computation*, vol. 35, pp. 93-110, 2017.
- [18] E. I. Batzelis, I. A. Routsolias, and S. A. Papanassiou, "An explicit PV string model based on the lambert W function and simplified MPP expressions for operation under partial shading," *IEEE Transactions on Sustainable Energy*, vol. 5, no. 1, pp. 301-312, 2013.
- [19] J. Bai, S. Liu, Y. Hao, Z. Zhang, M. Jiang, and Y. Zhang, "Development of a new compound method to extract the five parameters of PV modules," *Energy Conversion and Management*, vol. 79, pp. 294-303, 2014.
- [20] N. Femia, G. Petrone, G. Spagnuolo, and M. Vitelli, *Power electronics and control techniques for maximum energy harvesting in photovoltaic systems*. CRC press, 2017.
- [21] P. J. Gnetchejo, S. N. Essiane, A. Dadjé, and P. Ele, "A combination of Newton-Raphson method and heuristics algorithms for parameter estimation in photovoltaic modules," *Heliyon*, vol. 7, no. 4, pp. 66-73, 2021.
- [22] A. Harrag and S. Messalti, "Extraction of solar cell parameters using genetic algorithm," in *2015 4th International Conference on Electrical Engineering (ICEE)*, 2015, pp. 1-5: IEEE.
- [23] D. Allam, D. Yousri, and M. Eteiba, "Parameters extraction of the three diode model for the multi-crystalline solar cell/module using Moth-Flame Optimization Algorithm," *Energy Conversion and Management*, vol. 123, pp. 535-548, 2016.
- [24] D. H. Muhsen, A. B. Ghazali, T. Khatib, and I. A. Abed, "Extraction of photovoltaic module model's parameters using an improved hybrid differential evolution/electromagnetism-like algorithm," *Solar Energy*, vol. 119, pp. 286-297, 2015.
- [25] A. R. Jordehi, "Time varying acceleration coefficients particle swarm optimisation (TVACPSO): A new optimisation algorithm for estimating parameters of PV cells and modules," *Energy Conversion and Management*, vol. 129, pp. 262-274, 2016.
- [26] M. Abd Elaziz and D. Oliva, "Parameter estimation of solar cells diode models by an improved opposition-based whale optimization algorithm," *Energy conversion and management*, vol. 171, pp. 1843-1859, 2018.
- [27] A. Ayang et al., "Maximum likelihood parameters estimation of single-diode model of photovoltaic generator," *Renewable energy*, vol. 130, pp. 111-121, 2019.
- [28] A. Ayang et al., "Least square estimator and IEC-60891 procedure for parameters estimation of single-diode model of photovoltaic generator at standard test conditions (STC)," *Electrical Engineering*, vol. 103, no. 2, pp. 1253-1264, 2021.
- [29] N. F. Nicaire, P. N. Steve, N. E. Salome, and A. O. Grégoire, "Parameter Estimation of the Photovoltaic System Using Bald Eagle Search (BES) Algorithm," *International Journal of Photoenergy*, vol. 2021, 2021.
- [30] F. E. Ndi, S. N. Perabi, S. E. Ndjakomo, G. O. Abessolo, and G. M. Mengata, "Estimation of single-diode and two diode solar cell parameters by equilibrium optimizer method," *Energy Reports*, vol. 7, pp. 4761-4768, 2021.
- [31] L. Abualigah, "Multi-verse optimizer algorithm: a comprehensive survey of its results, variants, and applications," *Neural Computing and Applications*, vol. 32, no. 16, pp. 12381-12401, 2020.
- [32] D. Yousri et al., "Reliable applied objective for identifying simple and detailed photovoltaic models using modern metaheuristics: Comparative study," vol. 223, p. 113279, 2020.
- [33] P. J. Gnetchejo, S. N. Essiane, P. Ele, R. Wamkeue, D. M. Wapet, and S. P. Ngoffe, "Enhanced vibrating particles system algorithm for parameters estimation of photovoltaic system," *Journal of Power and Energy Engineering*, vol. 7, no. 08, p. 1, 2019.
- [34] L. H. I. Lim, Z. Ye, J. Ye, D. Yang, and H. Du, "A linear method to extract diode model parameters of solar panels from a single I-V curve," *Renewable Energy*, vol. 76, pp. 135-142, 2015.
- [35] M. Y. Javed et al., "A comprehensive review on a PV based system to harvest maximum power," *Electronics*, vol. 8, no. 12, p. 1480, 2019.
- [36] M. Calasan, S. H. A. Aleem, and A. F. Zobaa, "A new approach for parameters estimation of double and triple diode models of photovoltaic cells based on iterative Lambert W function," *Solar Energy*, vol. 218, pp. 392-412, 2021.
- [37] M. Calasan, S. H. A. Aleem, and A. F. Zobaa, "On the root mean square error (RMSE) calculation for parameter estimation of photovoltaic models: A novel exact analytical solution based on Lambert W function," *Energy conversion and management*, vol. 210, p. 112716, 2020.
- [38] Y. Feng, G.-G. Wang, S. Deb, M. Lu, and X.-J. Zhao, "Solving 0-1 knapsack problem by a novel binary monarch butterfly

- optimization," *Neural computing and applications*, vol. 28, pp. 1619-1634, 2017.
- [39] G. A. Breed, P. M. Seaverns, and A. M. Edwards, "Apparent power-law distributions in animal movements can arise from intraspecific interactions," *Journal of the Royal Society Interface*, vol. 12, no. 103, pp. 09-27, 2015.
- [40] E. Cuevas, M. A. Díaz Cortés, D. A. Oliva Navarro, E. Cuevas, M. A. Díaz Cortés, and D. A. Oliva Navarro, "A swarm global optimization algorithm inspired in the behavior of the social-spider," *Advances of Evolutionary Computation: Methods and Operators*, pp. 9-33, 2016.
- [41] J. James and V. O. Li, "A social spider algorithm for solving the non-convex economic load dispatch problem," *Neurocomputing*, vol. 171, pp. 955-965, 2016.
- [42] J. C. Choe and B. J. Crespi, *The evolution of social behaviour in insects and arachnids*. Cambridge University Press, 1997.
- [43] E. C. Yip, K. S. Powers, and L. Avilés, "Cooperative capture of large prey solves scaling challenge faced by spider societies," *Proceedings of the National Academy of Sciences*, vol. 105, no. 33, pp. 11818-11822, 2008.
- [44] M. Salomon, C. Sponarski, A. Larocque, and L. Avilés, "Social organization of the colonial spider *Leucauge* sp. in the Neotropics: vertical stratification within colonies," *The Journal of Arachnology*, vol. 38, no. 3, pp. 446-451, 2010.
- [45] A. Pasquet and B. Krafft, "Cooperation and prey capture efficiency in a social spider, *Anelosimus eximius* (Araneae, Theridiidae)," *Ethology*, vol. 90, no. 2, pp. 121-133, 1992.

VIII. TABLES

TABLE II. Comparison between the standard RMSE and the Lambert's RMSE for the SDM

Obj	Algorithms	I _{ph} (A)	I ₀ (μA)	R _s (Ω)	R _{sh} (Ω)	n	RMSE	RMSE Lambert
Obj1	SSO	0.7581225	0.5627167	0.0328821	40.9025725	1.5400682	0.0048977	-
	MBO	0.7607404	0.3631381	0.0359033	56.8404767	1.4930679	0.0010111	-
Obj2	SSO	0.7648172	0.8369124	0.0330777	48.6201192	1.5824912	-	0.00460517
	MBO	0.7608512	0.3286955	0.0362770	53.0088783	1.4829622	-	0.00078028

TABLE III. Comparison between the standard RMSE and the Lambert's RMSE for the DDM

Obj	Algorithms	I _{ph} (A)	I ₀₁ (μA)	R _s (Ω)	R _{sh} (Ω)	n ₁	I ₀₂ (μA)	n ₂	RMSE	RMSE Lambert (10 ⁻⁵)
Obj1	SSO	0.7600929	0.8745996	0.0358025	91.4723960	1.9938196	0.3188443	1.4866188	0.0063807	-
	MBO	0.7611615	0.5614189	0.0361921	52.8089084	1.7939177	0.1915798	1.4440137	0.0010652	-
Obj2	SSO	0.7601496	0.4496564	0.0294139	69.1354713	1.5867504	0.6478670	1.6432520	-	3.9434724
	MBO	0.7616087	0.2446412	0.0353916	47.8395571	1.4652683	0.4989489	1.8062628	-	0.63521313

TABLE IV. Comparison between the different extraction tools for SDM

Algorithms	I _{ph} (A)	I ₀ (μA)	R _S (Ω)	R _{Sh} (Ω)	n	RMSE Lambert
SSO	0.76481	0.83691	0.033077	48.6201	1.5824	0.00460517
MBO	0.76085	0.32869	0.036277	53.0088	1.4829	0.00078028
MPA [32]	0.76079	0.31072	0.036546	52.8871	1.4771	0.00077301
SMA [32]	0.76105	0.44962	0.034400	53.9823	1.5151	0.00117120
PPA [32]	0.76078	0.43557	0.034952	58.6694	1.5118	0.00095038
HHO [32]	0.76143	0.96500	0.031311	72.4432	1.6004	0.00216070

TABLE V. Comparison between the different extraction tools for DDM

Algorithms	I _{ph} (A)	I ₀₁ (μA)	R _S (Ω)	R _{Sh} (Ω)	n ₁	I ₀₂ (μA)	n ₂	RMSE Lambert (10 ⁻⁵)
SSO	0.7601496	0.4496564	0.0294139	69.1354713	1.5867504	0.6478670	1.6432520	3.9434724
MBO	0.76160	0.2446412	0.035391	47.8395	1.4652683	0.49894	1.8062628	0.63521313
MPA [32]	0.76080	0.11872	0.037419	55.4579	1.4011	0.92078	1.8505	76.965
SMA [32]	0.76035	0.31574	0.035155	67.4807	1.4846	0.84969	2	99.715
PPA [32]	0.76106	0.29966	0.034449	57.8076	1.4671	0.44560	1.7595	111.720
HHO [32]	0.76035	0.91286	0.034875	64.5645	1.8645	0.20341	1.4498	124.910
Chaotic LSHADE [36]	0.76076	0.20440	0.036907	55.5300	1.4424	0.87640	1.9952	75.274